# Effects of laser focusing properties on weldability in high-power fiber laser welding of thick high-strength steel plate

Cite as: J. Laser Appl. **29**, 012003 (2017); https://doi.org/10.2351/1.4966258
Submitted: 07 June 2016 • Accepted: 17 October 2016 • Published Online: 30 November 2016

**Naoyuki Matsumoto, Yousuke Kawahito, Koji Nishimoto, et al.**

# Effects of laser focusing properties on weldability in high-power fiber laser welding of thick high-strength steel plate

Naoyuki Matsumoto
*Graduate School of Engineering, Osaka University, 2-1 Yamadaoka, Suita, Osaka 565-0871, Japan*

Yousuke Kawahito
*Joining and Welding Research Institute, Osaka University, 11-1 Mihogaoka, Ibaraki, Osaka 567-0047, Japan*

Koji Nishimoto[a)]
*National Institute of Technology, Anan College, 265 Aoki Minobayashi, Anan, Tokushima 774-0017, Japan*

Seiji Katayama
*Joining and Welding Research Institute, Osaka University, 11-1 Mihogaoka, Ibaraki, Osaka 567-0047, Japan*

(Received 7 June 2016; accepted for publication 17 October 2016; published 28 October 2016)

The effect of various high-power laser-welding parameters on obtaining deep penetration welds without weld defects has been investigated. However, there are no studies on the effect of laser focusing. In this study, high-power fiber laser welding of a 12-mm-thick high-strength steel plate was performed by using two optics systems with different power density distributions and focus depths (2 or 4 mm) to investigate the effects of laser focusing properties on weldability. Full penetration welds without weld defects were obtained with the 4 mm focus depth optics system at low welding speeds of 25–50 mm/s. High-speed video and X-ray transmission images showed that the behavior of the molten pool on the top surface during laser welding was more stable for the 4 mm system than for the 2 mm system. The keyhole was stable with no large fluctuations, and no bubbles were formed in the keyhole. This result was attributed to keeping the power density within 50–120 kW/mm$^2$ to maintain a stable keyhole shape during the welding. Consequently, it was concluded that the laser-focusing properties during laser welding of a thick steel plate affected the weldability strongly, and the optics system with long focus depth was particularly useful in producing sound welds. © *2016 Laser Institute of America*. [http://dx.doi.org/10.2351/1.4966258]

Key words: high-power fiber laser, high-strength steel, laser focusing properties, weld penetration, molten pool, keyhole behavior

## I. INTRODUCTION

A high-brightness high-power fiber laser with a maximum power of 100 kW, a high lasing efficiency of about 20%, and a high beam quality of 2–12 mm•mrad has attracted intense interest for industrial applications where deep penetration welds in a thick steel or high-strength steel plate are required.[1–6] Recently, improvements in the cold crack resistance and toughness of the weld metal have allowed a high-strength thick steel plate to be used in various industrial areas such as spherical gas tanks, bridges, hydraulic pressure iron pipes, ocean structures, and construction.[7–9] It is expected that high-speed deep penetration welding of a thick high-strength steel plate can be achieved by the latest advances in the development of a high-power fiber laser. However, high-power fiber laser welding of a thick metal plate, such as stainless steel, steel, and aluminum alloys, has been performed to investigate the effects on weldability of laser-welding parameters, such as laser power, focus distance, welding speed, shielding gas, and beam spot diameter, and of material parameters, such as gap tolerance, surface preparation, and filler materials.[10–17] For example, Kawahito *et al.*[10] investigated the effects of laser power, power density, and welding speed on the formation of sound welds between thick stainless steel plate by high-power fiber laser welding with spot diameters of 130, 200, 360, and 560 $\mu$m. The laser power density had a strong effect on the increase in weld penetration depth as welding speed increased, and sound partially penetrated welds with no weld defects, like underfill, undercut, humps, and porosity, were produced at welding speeds from 75 to 167 mm/s and spot diameters of 360 or 560 $\mu$m. Sokolov and Salminen[15] examined the effects of joint edge surface roughness and the air gap between the specimens on penetration depth during high-power fiber laser welding of low alloyed steels. Edge surface preparation to a roughness of about Ra 6.3 $\mu$m with an air gap of 0.1–0.2 mm resulted in deeper penetration welds and better weldability. However, there are no studies of the effects on weldability of laser focusing properties such as power density according to focus distance, spot diameter, and focus depth during laser welding of a thick metal plate.

In this work, high-power fiber laser welding of a 12-mm-thick high-strength steel plate was performed with two optics systems with different focusing properties to investigate

[a)]Author to whom correspondence should be addressed; electronic mail: knishi@anan-nct.ac.jp. Telephone: +81-884-23-7160

 

weldability and behavior of the molten pool and keyhole during laser welding. The effects of laser focusing properties on weld defects, such as underfill, humps, spatter, and porosity, and on penetration depth were investigated. To clarify the welding phenomena arising during high-power fiber laser welding of a thick steel plate, the dynamics of melt flows in the molten pool on the top surface of the specimen and the keyhole behavior affecting porosity formation during the welding were analyzed by using a high-speed video camera and an *in situ* microfocused X-ray transmission system, respectively.

## II. MATERIALS AND EXPERIMENTAL PROCEDURES

The material used in high-power fiber laser welding experiments was 780 MPa high-strength steel with a thickness of 12 mm. Figure 1 shows a schematic diagram of the experimental setup for high-power fiber laser welding of a high-strength steel plate. A high-brightness high-power continuous wave fiber laser with a maximum power of 10 kW and a wavelength of 1070 nm was used. The laser beam with a 4.5 mm·mrad beam parameter product was delivered through the optical fiber of 100 $\mu$m core diameter. Figure 2 shows the focusing properties, laser beam profiles, and focus depths of two different optics systems used in the laser welding experiments. For the normal optics system (optics system A), the spot diameter was 200 $\mu$m at the focal point and the focus depth was 2 mm, and those of the optics system with long focus depth (optics system B) were 270 $\mu$m and 4 mm, respectively. When the beam diameter before (+) and after (–) the focal point in the laser propagation direction was diffused up to $\sqrt{2}$ times the spot diameter, the focus distance measured was defined as the focus depth. The focus depth of optics system B was twice that of optics system A. The incident angle ($\theta$) of the fiber laser head was tilted forward 10° to avoid back-reflection in the fiber laser head. High-power fiber laser welding of a high-strength thick steel plate was conducted by changing the welding speed ($v$) from 25 to 167 mm/s at a laser power ($p$) of 10 kW and a focal point of 0 mm. The Ar shielding gas of 40 l/min was supplied from an 8-mm-diameter gas nozzle mounted at 45° to suppress the oxidation of weld beads. The behavior of the molten pool on the top surface of the steel plate during laser welding using optics systems A and B was observed by a high-speed video camera. The laser-irradiated part was observed at a frame rate of 10 000 frame/s by using a spectral filter with a wavelength of 974.5 ± 7.7 nm under diode laser illumination with a wavelength of 980 nm and a maximum power of 30 W. The keyhole behavior, the porosity, and the mechanism of porosity formation in the keyhole during high-power fiber laser welding with optics systems A and B were visibly confirmed by using the microfocused X-ray transmission *in situ* observation system at a frame rate of 250 frame/s, as shown in Fig. 3. The specimens used for X-ray transmission *in situ* observation were 3 mm wide and 12 mm thick.

## III. RESULTS AND DISCUSSION

### A. Effects of laser focusing properties on weldability

High-power fiber laser welding experiments for a 12-mm-thick high-strength steel plate were conducted with optics systems A and B. Figure 4 shows the top surface appearance, weld beads, and X-ray transmission results of cross sections of the welds obtained by optics system A with a 2 mm focus depth. The laser welding experiments were performed at welding speeds of 25–167 mm/s at a laser power of 10 kW. A full penetration weld could be produced at a welding speed of 25 mm/s only, but deep underfill weld defects were generated on the top or bottom surface of the weld beads. In addition, submillimeter porosities in the weld bead on the longitudinal side in the welding direction were observed by X-ray transmission analysis. For welding speeds greater than 50 mm/s, partial penetration welds were produced, and humps were formed on the top surface of the welds. The humps were generated at a small spot diameter of 200 $\mu$m and higher welding speeds, as reported by Kawahito *et al.*[10,11] Moreover, the weld width became narrower and the penetration depth became shallower with the increase in the welding speed, and the X-ray transmission analysis showed that porosities in the longitudinal welds were present around the tip of the keyhole. Figure 5 shows the top surface appearance, weld beads, and X-ray transmission results for

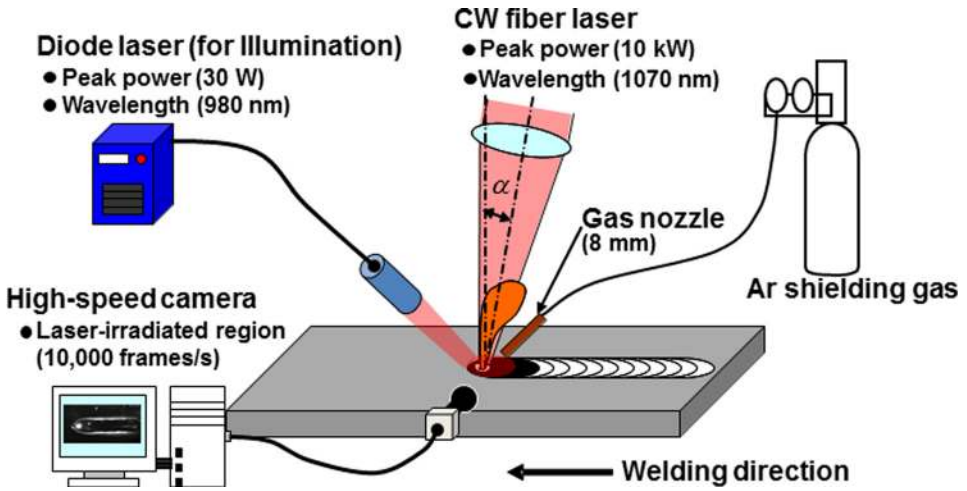


FIG. 1. Schematic of the experimental setup during high-power fiber laser welding of a high-strength steel.

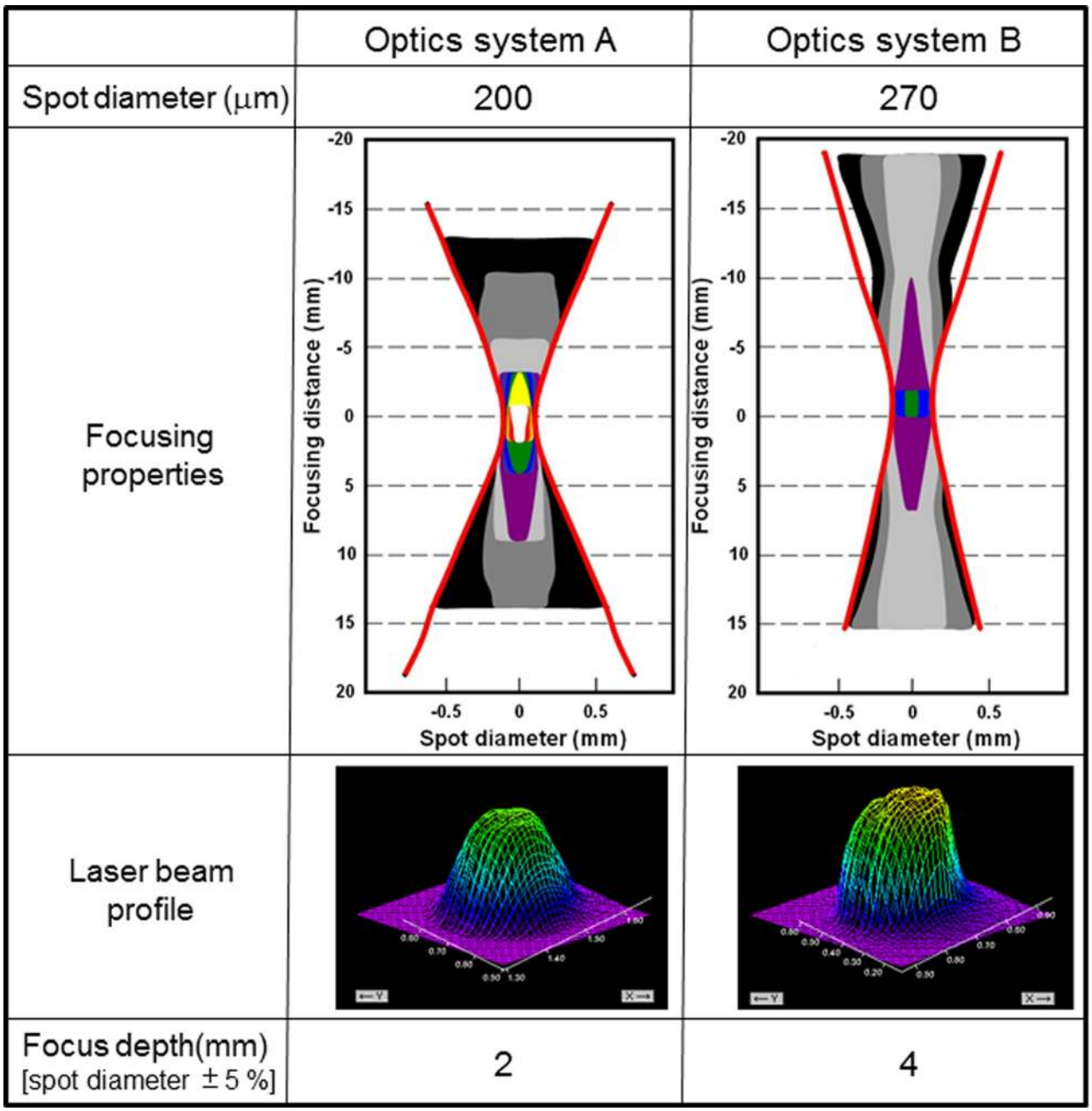


FIG. 2. Spot diameter, focusing properties, laser beam profiles, and focus depth of optics systems A and B.

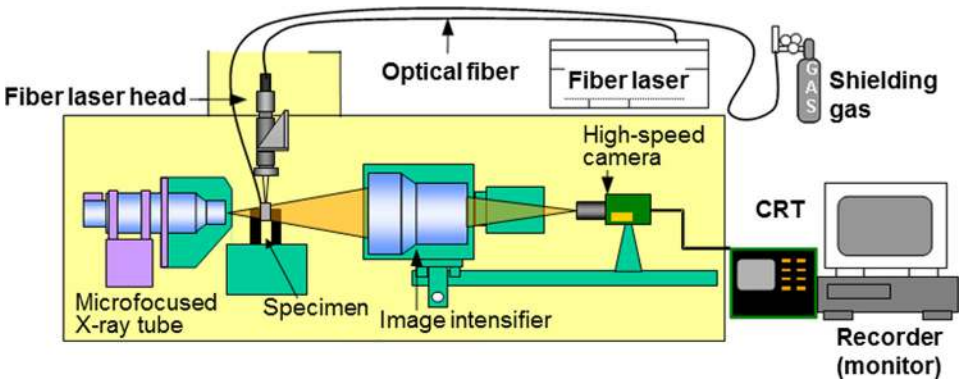


FIG. 3. Schematic of the microfocused *in situ* X-ray transmission system.

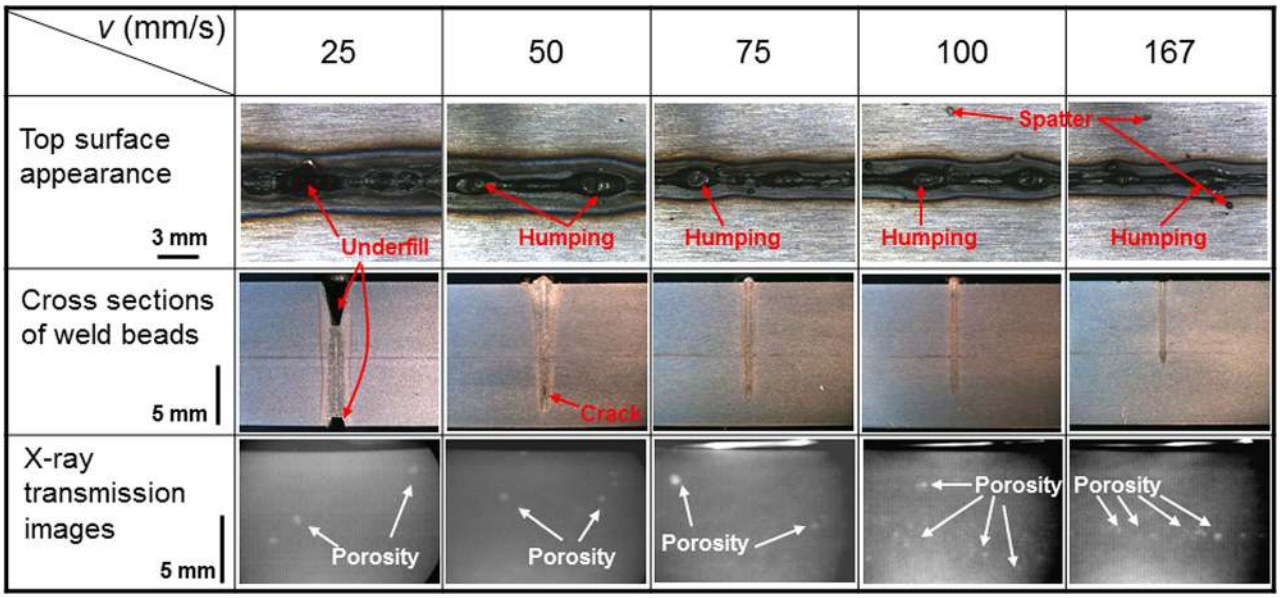


FIG. 4. Top surface appearance, weld beads, and X-ray transmission analysis of cross sections for welds obtained by fiber laser welding of a high-strength steel with optics system A (2 mm focus depth).

the cross sections of the welds obtained by fiber laser welding with optics system B with a 4 mm focus depth. Full penetration welds were produced at welding speeds of 25 and 50 mm/s, and no defects were generated on the top surfaces and cross sections of the welds. In particular, at a welding speed of 25 mm/s, a sound weld with no porosity inside the weld bead was achieved. At welding speeds of greater than 75 mm/s, partially penetrated welds were produced, and the weld width of the top surfaces became narrower and the penetration depth of the cross sections became shallower, similar to the results for optics system A at welding speeds greater than 50 mm/s. At welding speeds of 100 and 167 mm/s, X-ray transmission analysis showed that spatter was formed on the top surfaces of the welds, and the porosity around the tip of keyhole was high compared with low welding speeds of 25–50 mm/s. In addition, a shallow underfill was produced on the top surface of the weld at a welding speed of 167 mm/s.

The effects of focusing properties on penetration depth during laser welding were examined in detail (Fig. 6). For optics system B with a 4 mm focus depth, full penetration welds were achieved at welding speeds of 16–50 mm/s, and the penetration depth increased slightly compared with optics system A with a 2 mm focus depth. It has been reported that full penetration welds of 12-mm-thick high-strength steel plate may be possible because a power density higher than the critical power density of about 12 kW/mm$^2$ is necessary to produce a keyhole with a high depth-to-width ratio[18,19] that reaches the bottom surface of steel plate, as

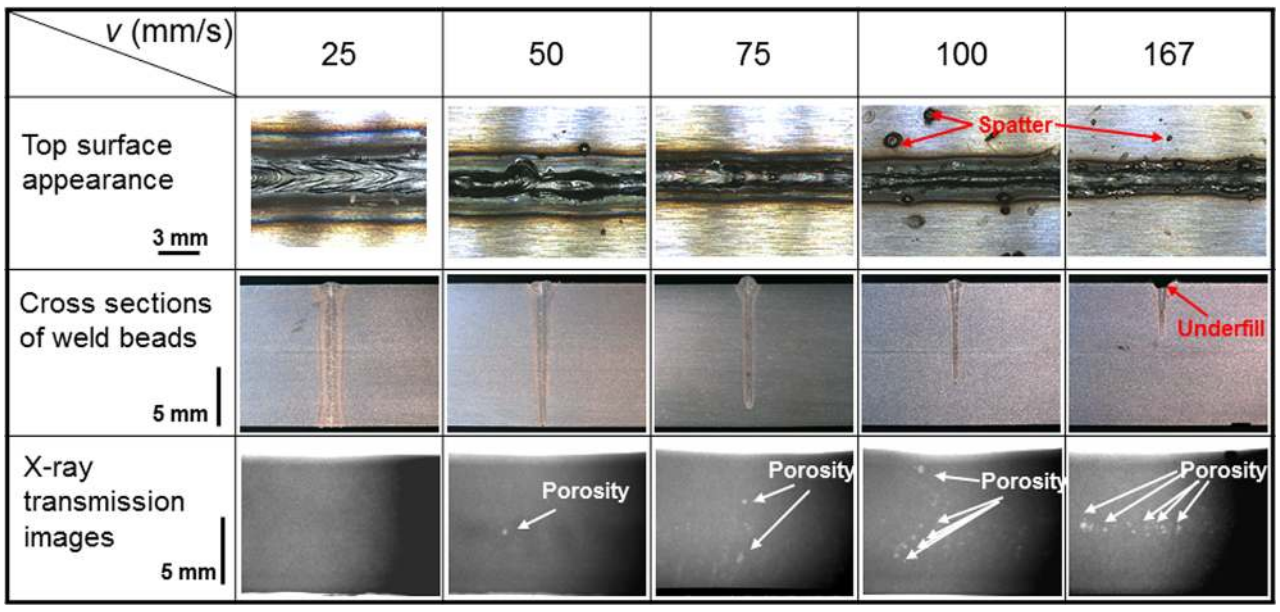


FIG. 5. Top surface appearance, weld beads, and X-ray transmission analysis of cross sections obtained by fiber laser welding of a high-strength steel with optics system B (4 mm focus depth).

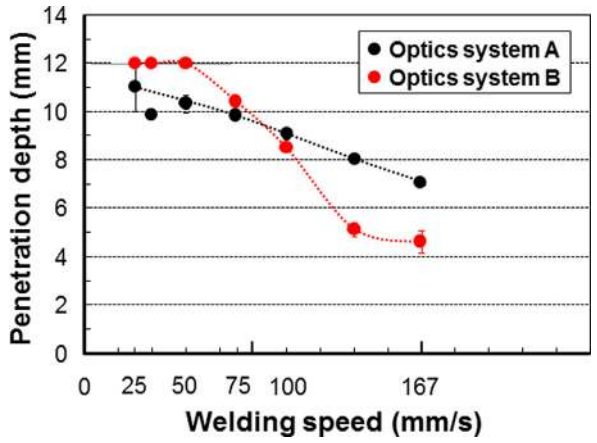


FIG. 6. Penetration depth vs welding speed for optics systems A and B.

shown in Fig. 7. The peak power density of optics systems A and B at a depth of 10 mm were about 50 and 32 kW/mm$^2$, respectively. At welding speeds from 75–100 mm/s, the penetration depth of optics A and B were similar. In contrast to optics system A, the penetration depth of optics system B at welding speeds of 133–167 mm/s decreased sharply and was much lower than at 3–3.5 mm. The deeper penetration depth of optics system A at higher welding speeds arose from the increase in laser heat input ($p/v$) caused by the higher peak power density near the focal point compared with the low peak power density of optics system B. Laser heat input was inversely proportional to the welding speed. Consequently, we concluded that the laser focusing properties in high-power fiber laser welding of a thick steel plate affected the weldability. In particular, the optics system with a 4 mm focus depth was better than the optics system with a 2 mm focus depth at low welding speeds to accomplish sound welds without weld defects, although partial penetration welds were produced at higher welding speeds.

### B. Dynamics of molten pool and keyhole behavior affecting porosity formation

To clarify the effects of the laser focusing properties of optics systems A and B on weldability, the dynamics of melt flows in the molten pool on the top surface of the steel plate during laser welding were investigated by a high-speed video camera. Figures 8 and 9 show high-speed video images of the molten pool during welding with optics systems A and B, respectively. The welding conditions were a laser power of 10 kW and a welding speed of 25 mm/s. In Fig. 8, the molten pool in fiber laser welding with optics system A fluctuated violently, and the weld metal at the rear end of the molten pool billowed forming weld defects like humps. Moreover, weld beads with unstable shapes, including underfills, were generated, and spatter from the molten pool of the keyhole entrance was observed. These observations were explained by excessive laser heat input at low welding speed caused by higher peak power density with a small spot diameter of 200 $\mu$m. In contrast, for optics system B (Fig. 9), the molten pool during laser welding was stable, and sound weld beads without weld defects, such as underfill or spatter, were produced. Moreover, the length of the molten pool (5.6 mm) was slightly longer than that for optics system A (5.0 mm), and the solidified shape at the rear end of the molten pool was desirable and underwent a stable solidification process.

Next, the effect of laser focusing properties on the keyhole behavior and the mechanisms of porosity formation in the keyhole during welding were examined. Figures 10 and 11 show *in situ* X-ray transmission images obtained during laser welding of high-strength steel with optics systems A and B, respectively. The welding conditions were a laser power of 10 kW and a welding speed of 25 mm/s. In Fig. 10, the keyhole generated with optics system A fully penetrated to the bottom surface of the steel plate, although the keyhole during laser irradiation was periodically unstable and fluctuated violently. Porosity arose from a big bubble that formed near the middle side of the keyhole and became trapped at the solidifying front of the weld fusion zone. This was explained by the formation of a keyhole with a wide, unstable shape (Fig. 12(a)) because of the concentrated distribution of power density within 180–210 kW/mm$^2$ in the middle point of the keyhole during the welding. In contrast, for optics system B, the keyhole during laser irradiation fully penetrated to the bottom surface of the thick steel plate and was stable with no intense fluctuations, and no bubbles were formed in the keyhole. This was explained by the power density of 50–120 kW/mm$^2$, which generated a stable keyhole (Fig. 12(b)). Consequently, sound welds with a stable keyhole and no porosity were obtained by high-power fiber laser welding by using an optics system with a long focus depth because the system supplied a balanced power density.

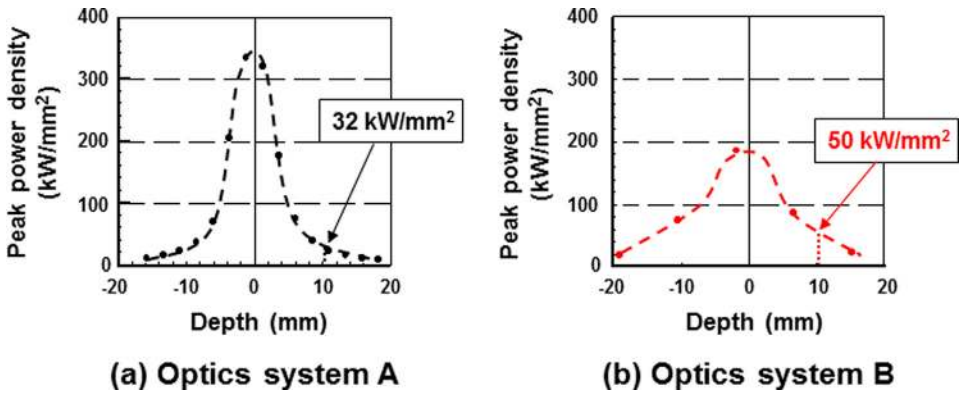


FIG. 7. Peak power density vs depth for optics systems (a) A and (b) B.

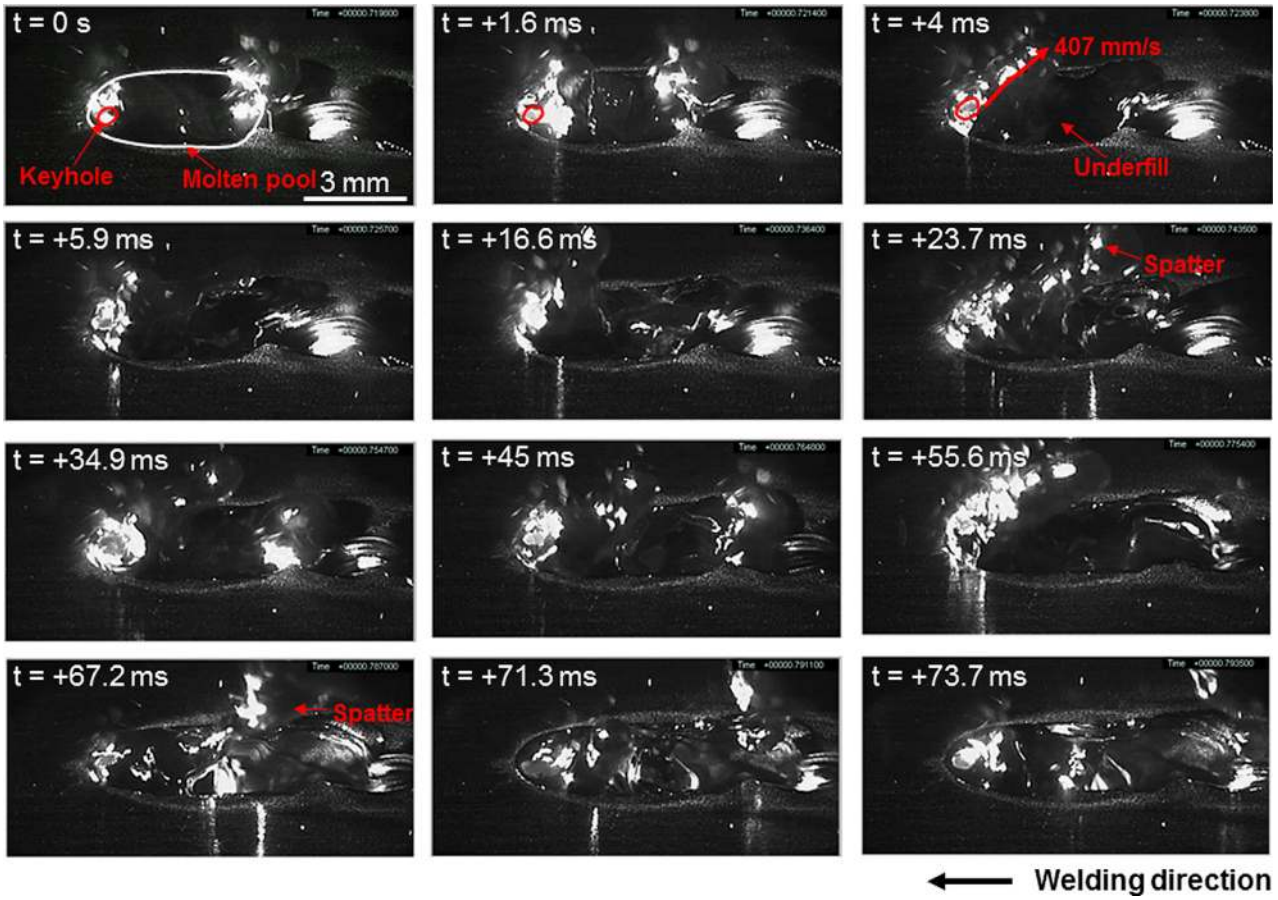


FIG. 8. High-speed video images of the molten pool during high-power fiber laser welding of a high-strength steel with optics system A (2 mm focus depth), showing unstable melt flow, underfill, and spatter generation in the molten pool.

## IV. CONCLUSIONS

High-power fiber laser welding of a 780 MPa high-strength steel plate with a thickness of 12 mm was performed with optics systems A and B with different focusing properties. For optics system B, which had a 4 mm focus depth and 270 $\mu$m spot diameter, fully penetrated welds with no weld defects, such as underfill, humps, and porosity, were produced at welding speeds of 25–50 mm/s compared with optics system A, which had a 2 mm focus depth and 200 $\mu$m spot diameter. However, at higher welding speeds of 133–167 mm/s, optics system A had a deeper penetration depth than optics system B because optics system A had a higher peak power density near the focal point. The high-speed video observation and *in situ* X-ray transmission images during laser welding demonstrated that melt flows in the molten pool observed in laser welding of optics system B were stable compared with optics system A. The instability

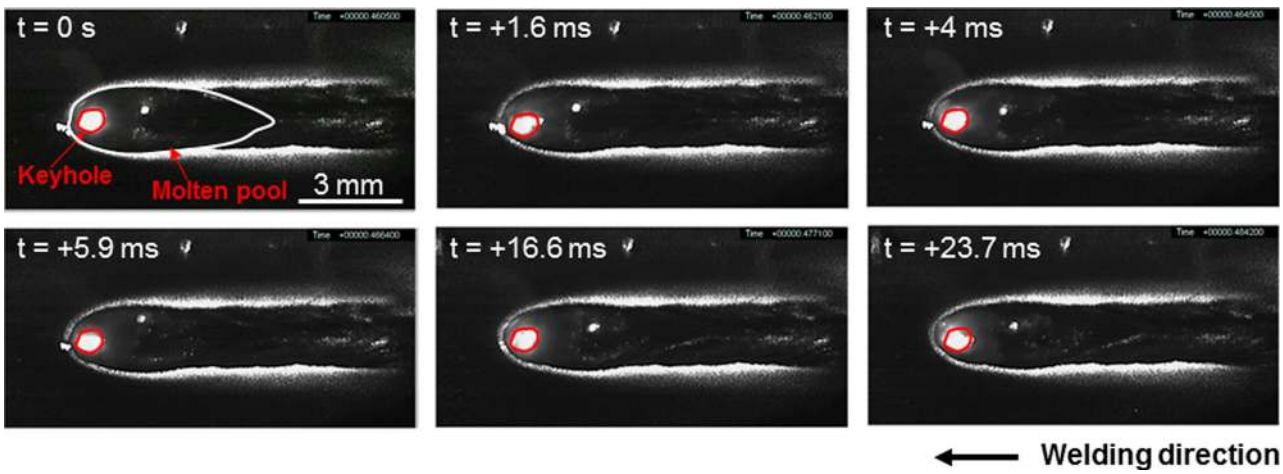


FIG. 9. High-speed video images of the molten pool during high-power fiber laser welding of a high-strength steel using optics system B (4 mm focus depth), showing stable melt flow in the molten pool.

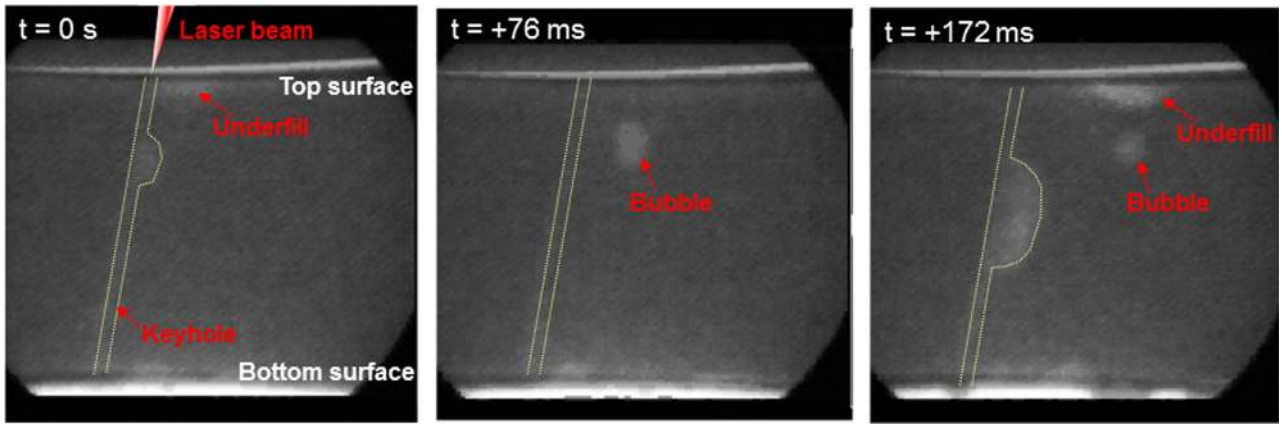


FIG. 10. *In situ* X-ray transmission images during high-power fiber laser welding with optics system A showing unstable keyhole behavior and bubble formation.

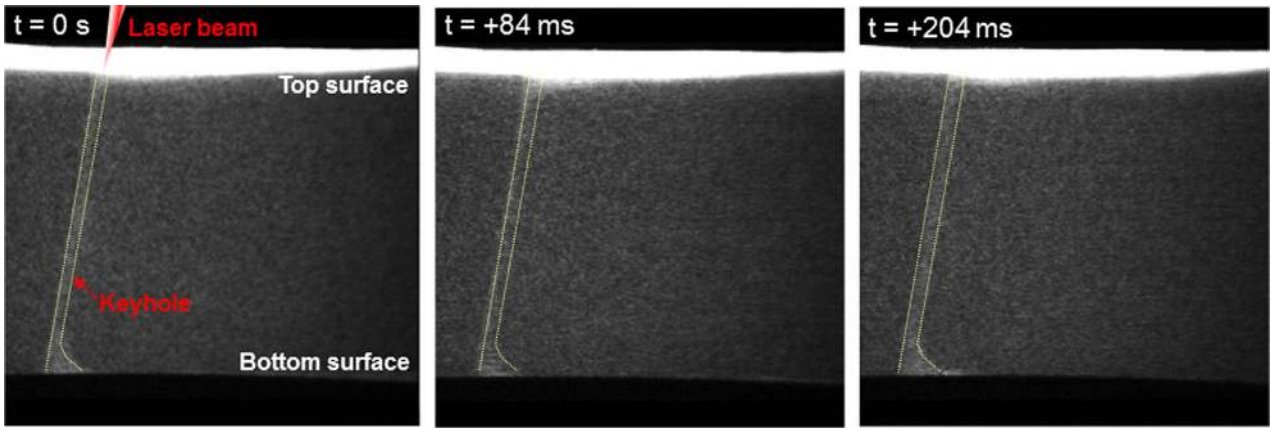


FIG. 11. *In situ* X-ray transmission images during high-power fiber laser welding with optics system B showing stable keyhole behavior and no bubbles.

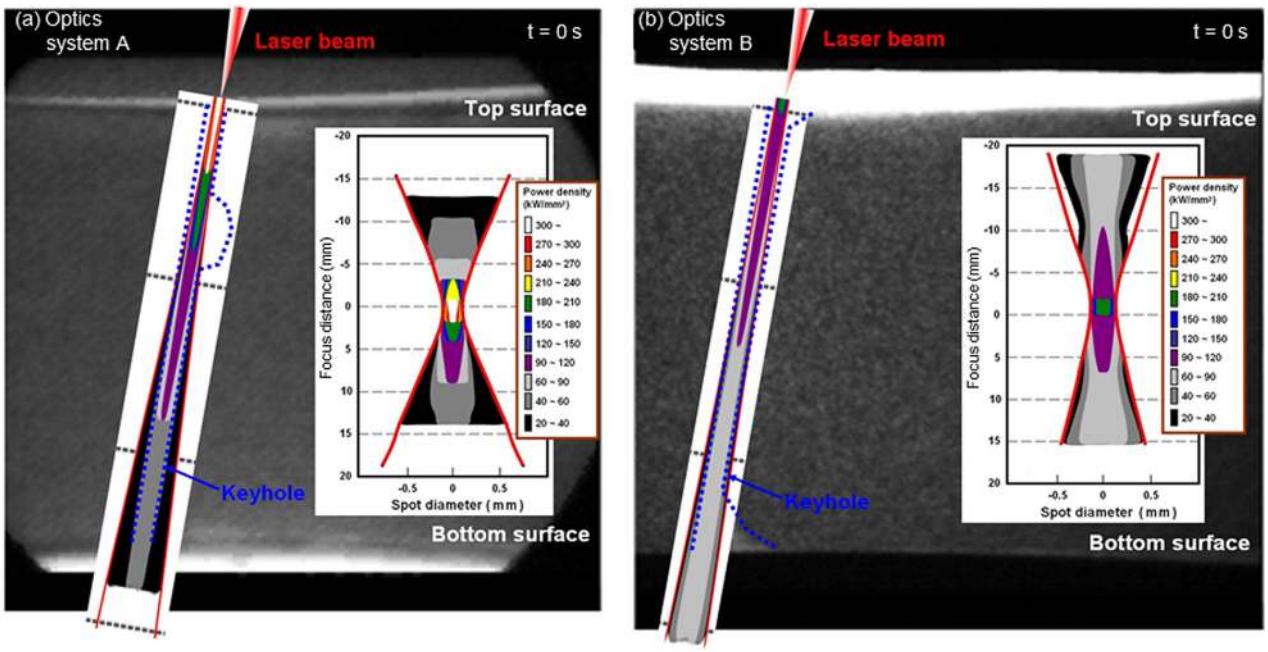


FIG. 12. Comparison of the relationship between keyhole shape and laser power density during laser welding with optics systems (a) A and (b) B.

produced by optics system A resulted in underfill and spatter. For optics system B, the stable keyhole fully penetrated to the bottom surface of a thick steel plate, and no bubbles were formed. The power density within 50–120 $kW/mm^2$ necessary for maintaining a stable keyhole shape was continuously supplied. Therefore, considering the effect of laser focusing properties on high-power laser welding of a thick metal plate should contribute to the development of welding technology.

[1]N. Seto, S. Katayama, and A. Matsunawa, "High-speed simultaneous observation of plasma and keyhole behavior during high power $CO_2$ laser welding: Effect of shielding gas on porosity formation," J. Laser Appl. **12**, 245–250 (2000).
[2]Y. Shimokusu, S. Fukumoto, M. Nayama, T. Ishide, S. Tsubota, A. Matsunawa, and S. Katayama, "Application of 7 kW class high power yttrium-aluminum-garnet laser welding to stainless steel tanks," J. Laser Appl. **14**, 68–72 (2002).
[3]X. B. Liu, G. Yu, M. Pang, J. W. Fan, H. H. Wang, and C. Y. Zheng, "Dissimilar autogenous full penetration welding of superalloy K418 and 42CrMo steel by a high power CW Nd:YAG laser," Appl. Surf. Sci. **253**, 7281–7289(2007).
[4]G. Li, Y. Cai, and Y. Wu, "Stability information in plasma image of high power $CO_2$ laser welding," Opt. Lasers Eng. **47**, 990–994 (2009).
[5]L. Quintino, A. Costa, R. Miranda, D. Yapp, V. Kumar, and C. J. Kong, "Welding with high power fiber lasers—A preliminary study," Mater. Des. **28**, 1231–1237 (2007).
[6]Y. Kawahito, T. Ohnishi, and S. Katayama, "In-process monitoring and feedback control for stable production of full-penetration weld in continuous wave fibre laser welding," J. Phys. D. Appl. Phys. **42**, 085501 (2009).
[7]C. Miki, K. Homma, and T. Tominaga, "High strength and high performance steels and their use in bridge structures," J. Constr. Steel. Res. **58**, 3–20 (2002).
[8]W. H. Sun, G. D. Wang, J. M. Zhang, and D. X. Xia, "Microstructure transformation behavior of 610 MPa HSLA steel plate for 150 000 $m^3$ oil storage tank construction," Int. J. Iron Steel Res. **17**, 48–52 (2010).
[9]Y. Yang, T. Zhang, Y. Shao, G. Meng, and F. Wang, "Effect of hydrostatic pressure on the corrosion behaviour of Ni-Cr-Mo-V high strength steel," Corrosion Sci. **52**, 2697–2706 (2010).
[10]Y. Kawahito, M. Mizutani, and S. Katayama, "Elucidation of high-power fibre laser welding phenomena of stainless steel and effect of factors on weld geometry," J. Phys. D: Appl. Phys. **40**, 5854–5859 (2007).
[11]Y. Kawahito, K. Kinosita, N. Matsumoto, M. Mizutani, and S. Katayama, "Effect of weakly ionised plasma on penetration of stainless steel weld produced with ultra high power density fibre laser," Sci. Technol. Weld. Join. **13**, 749–753 (2008).
[12]Y. Kawahito, N. Matsumoto, Y. Abe, and S. Katayama, "Relationship of laser absorption to keyhole behavior in high power fiber laser welding of stainless steel and aluminum alloy," J. Mater. Process. Technol. **211**, 1563–1568 (2011).
[13]J. Wang, C. Wang, X. Meng, X. Hu, Y. Yu, and S. Yu, "Study on the periodic oscillation of plasma/vapour induced during high power fibre laser penetration welding," Opt. Laser Technol. **44**, 67–70 (2012).
[14]M. J. Zhang, G. Y. Chen, Y. Zhou, S. C. Li, and H. Deng, "Observation of spatter formation mechanisms in high-power fiber laser welding of thick plate," Appl. Surf. Sci. **280**, 868–875 (2013).
[15]M. Sokolov and A. Salminen, "Experimental investigation of the influence of edge morphology in high power fiber laser welding," Phys. Procedia **39**, 33–42 (2012).
[16]M. Sokolov, A. Salminen, M. Kuznetsov, and I. Tsibulskiy, "Laser welding and weld hardness analysis of thick section S355 structural steel," Mater. Des. **32**, 5127–5131 (2011).
[17]R. Miranda, A. Costa, L. Quintino, D. Yapp, and D. Iordachescu, "Characterization of fiber laser welds in X100 pipeline steel," Mater. Des. **30**, 2701–2707 (2009).
[18]G. Herziger, *The Industrial Laser Annual Handbook*, edited by D. Belforte and M. Levitt (Pennwell Books, Tulsa, OK, 1986), pp. 108–115.
[19]E. A. Metzbower, "Keyhole formation," Metall. Mater. Trans. B **24**, 875–880 (1993).